



# Efficacy of Combination Neoadjuvant Chemotherapy and Regional Inductive Moderate Hyperthermia in the Treatment of Patients With Locally Advanced Breast Cancer

Technology in Cancer Research & Treatment  
Volume 19: 1-10  
© The Author(s) 2020  
Article reuse guidelines:  
sagepub.com/journals-permissions  
DOI: 10.1177/1533033820963599  
journals.sagepub.com/home/tct  


Anton Loboda, MD, PhD<sup>1</sup>, Ivan Smolanka Sr, MD<sup>1</sup>,  
Valerii E. Orel, DSc<sup>1,2</sup> , Liubov Syvak, MD<sup>1</sup>, Tetiana Golovko, MD<sup>1</sup>,  
Iryna Dosenko, MD, PhD<sup>1</sup>, Andrii Lyashenko, MD, PhD<sup>1</sup>,  
Ivan Smolanka Jr, MD<sup>1</sup>, Olha Dasyukevich, PhD<sup>1</sup>,  
Tetiana Tarasenko, MD<sup>1</sup>, Valerii B. Orel, MD<sup>1</sup>, Alex Rykhalskyi, MSc<sup>1</sup>,  
Oleksandr Ganich, MD<sup>1</sup>, and Oleksandr Mokhonko, BEng<sup>2</sup>

## Abstract

**Purpose:** To evaluate the efficacy of neoadjuvant chemotherapy in combination with regional inductive moderate hyperthermia for patients with locally advanced breast cancer. **Patients and Methods:** 200 patients with stage IIB-IIIa breast cancer received neoadjuvant chemotherapy (control group, n = 97) or chemotherapy combined with hyperthermia (experimental group, n = 103). Inductive hyperthermia was set at  $27.12 \pm 0.16$  MHz and the 50 W output power. **Results:** Thermal and color Doppler ultrasound imaging demonstrated that hyperthermia increased the surface temperature on the breasts to  $< 4^\circ\text{C}$  while the mean values for systolic blood flow were 3.5 times as high as those prior to treatment. Assessment of tumor size and response found a  $(31.24 \pm 3.85)\%$  reduction in the size of the primary tumor in patients receiving chemotherapy + hyperthermia, while chemotherapy alone showed a  $(22.95 \pm 3.61)\%$  decrease on average ( $p = 0.034$ ). The rate of objective response increased by 15.9% in the experimental group ( $p = 0.034$ ) compared with the control group. The patients in the experimental group also had axillary lymph node regression of 14.17% greater than in the control group ( $p = 0.011$ ). Moreover, the combination treatment allowed to increase the proportion of women eligible for breast-conserving and reconstructive surgery by 13.63% in the experimental group. The viable tumor volume was lower in patients receiving neoadjuvant chemotherapy + hyperthermia ( $24.4 \pm 0.2\%$ ) compared with those given chemotherapy alone ( $30.4 \pm 0.25\%$ ). The 10-year overall survival rates were higher (log-rank:  $p = 0.009$ ) in breast cancer patients who underwent chemotherapy combined with hyperthermia than in patients receiving chemotherapy only. **Conclusion:** The combination neoadjuvant chemotherapy and the technology of regional inductive moderate hyperthermia improved the efficacy of treatment for patients with locally advanced breast cancer staged IIB-IIIa.

## Keywords

breast cancer, chemotherapy, inductive hyperthermia, computer-assisted treatment planning, combination treatment

## Abbreviations

BC, Breast cancer; CT, Computed tomography; CTCAE v4.03, Common Terminology Criteria for Adverse Events version 4.03; ECOG, Eastern Cooperative Oncology Group; FAC, 5-fluorouracil, doxorubicin, cyclophosphamide; HER-2, Human epidermal

<sup>1</sup> National Cancer Institute, Kyiv, Ukraine

<sup>2</sup> Biomedical Engineering Department, "Igor Sikorsky Kyiv Polytechnic Institute," Kyiv, Ukraine

## Corresponding Author:

Valerii E. Orel, Medical Physics and Bioengineering Research Laboratory, National Cancer Institute, 33/43 Lomonosov Str., 03022, Kyiv, Ukraine.  
Email: valeriiorel@gmail.com



growth factor 2 receptor; ICD-O-3, International Classification of Diseases for Oncology 3rd Edition; MRI, Magnetic resonance imaging; NACT, Neoadjuvant chemotherapy; NCCN, National Comprehensive Cancer Network; NCI, National Cancer Institute of Ukraine; RECIST 1.0, Response evaluation criteria in solid tumors v 1.0; RIMH, Regional inductive moderate hyperthermia; ROS, Reactive oxygen species; SAR, Specific absorption rate; US, Ultrasound

Received: May 16, 2020; Revised: July 27, 2020; Accepted: August 19, 2020.

## Introduction

Breast cancer (BC) poses the ongoing challenge of improving diagnosis and treatment for healthcare and society. BC is the leading cause of death in women and is responsible for 15% of cancer-related deaths globally. Women of reproductive age have not considered themselves to be at risk for BC previously. However, the disease also affects younger women who could benefit from breast conservation therapy. While most countries report the increase in BC incidence, the death rates continue to decline.<sup>1,2</sup>

BC is a heterogeneous disease with distinct molecular, redox, genetic, histological and clinical signatures between tumors originating from the epithelium lining the milk ducts and lobules of the breast.<sup>3</sup> The heterogeneous nature of the redox signaling contributes to tumor adaptation and the development of aggressive BC resistance to treatment.<sup>4</sup> Cancer cells generally exhibit higher oxidative stress than normal cells. Not only do elevated levels of reactive oxygen species (ROS) damage DNA, induce mutations needed to drive tumor initiation and progression, but also much of research attention has been drawn to redox targeted strategies for BC treatment.<sup>5,6</sup>

Despite potential side-effects, chemo-, radiotherapy and breast surgery are the preferred treatment for most women. In the past 3 decades, surgical treatment of the primary tumor has shifted toward breast conservation techniques that preserve the appearance and function of the breast. The combination of breast-conserving surgery and other treatment modalities improves long-term survival.<sup>7</sup>

Cardiotoxicity associated with chemo- and radiotherapy involves ROS-mediated signaling and damage. BC patients who have undergone neoadjuvant chemotherapy (NACT) may be at higher risk of cardiovascular mortality.<sup>8</sup> The proposed mechanism by which many chemotherapeutic agents, such as doxorubicin in combination with 5-fluorouracil and cyclophosphamide—FAC regimen, act in the tumor cell is based on pro-oxidant effects. An additional increase in ROS levels triggers preferential killing of tumor cells, whereas normal cells are more likely to upregulate antioxidant defense responses to cope with oxidative stress. Further clinical data collection is required to determine exactly how pro-oxidant therapy affects BC prognosis.<sup>9</sup>

The use of combined radiofrequency hyperthermia, chemotherapy and/or radiotherapy provides proven benefit to patients with BC in the neoadjuvant, definitive and adjuvant setting. The mechanism underlying biological interactions with the electromagnetic field involves spin conversion in free

radical pairs. The change in the balance between triplet and singlet state probabilities in favor of the latter promotes ROS generation and oxidative stress.<sup>10</sup> Previously, our experimental investigation has indicated that inductive moderate hyperthermia combined with anthracyclines initiates oxidative stress damage to cancer cells.<sup>11</sup>

Regional inductive moderate hyperthermia (RIMH) is a treatment modality for locally advanced and metastatic BC where time-varying magnetic fields induce eddy currents to heat (< 42°C) and alter the redox state of the tumor and/or metastasis. Recent evidence suggests that even a moderate temperature rise can cause redox-mediated changes in the tumor during RIMH. Since electromagnetic radiation can act on anticancer drugs with the free radical mechanism, the activity of these agents is modulated in the tumor area exposed to RIMH.<sup>12-15</sup> Failure of antioxidant systems to protect against elevated levels of ROS, i.e. lipid peroxidation, protein damage, leads to tumor cell death.<sup>16</sup> RIMH technology could introduce a personalized approach for NACT by increasing the efficacy of anticancer drugs given before breast-conserving and reconstructive surgery.

This paper is a continuation of previous work designed to compare NACT versus NACT and RIMH in BC patients with multiple liver metastases.<sup>17</sup> The present study examines the application of RIMH to improve the antitumor efficacy of NACT followed by breast-conserving and reconstructive surgery in patients with locally advanced BC.

## Patients and Methods

### Patients

Eligible women patients, aged  $\geq 18$ , had a histological diagnosis of invasive unilateral BC with (T2N1M0, T3N0M0, T1N2aM0, T2N2aM, T3N1M0, T3N2aM0) stage and an Eastern Cooperative Oncology Group (ECOG) performance status of 0-2. All patients had a clear indication for neoadjuvant therapy and provided written informed consent for RIMH. Research procedures were performed in accordance with the Declaration of Helsinki and approved by the Regional Committee for Medical Research Ethics of National Cancer Institute of Ukraine (NCI) protocol No. 63.

Patients were excluded if they were pregnant, breastfeeding, had a serious concomitant disorder (stage 3 congestive heart failure, liver or kidney failure, etc.) or any malignancy other than BC.

Participants were randomly assigned to the experimental (neoadjuvant FAC + RIMH) group or the control group (neoadjuvant FAC). Baseline assessment included bilateral

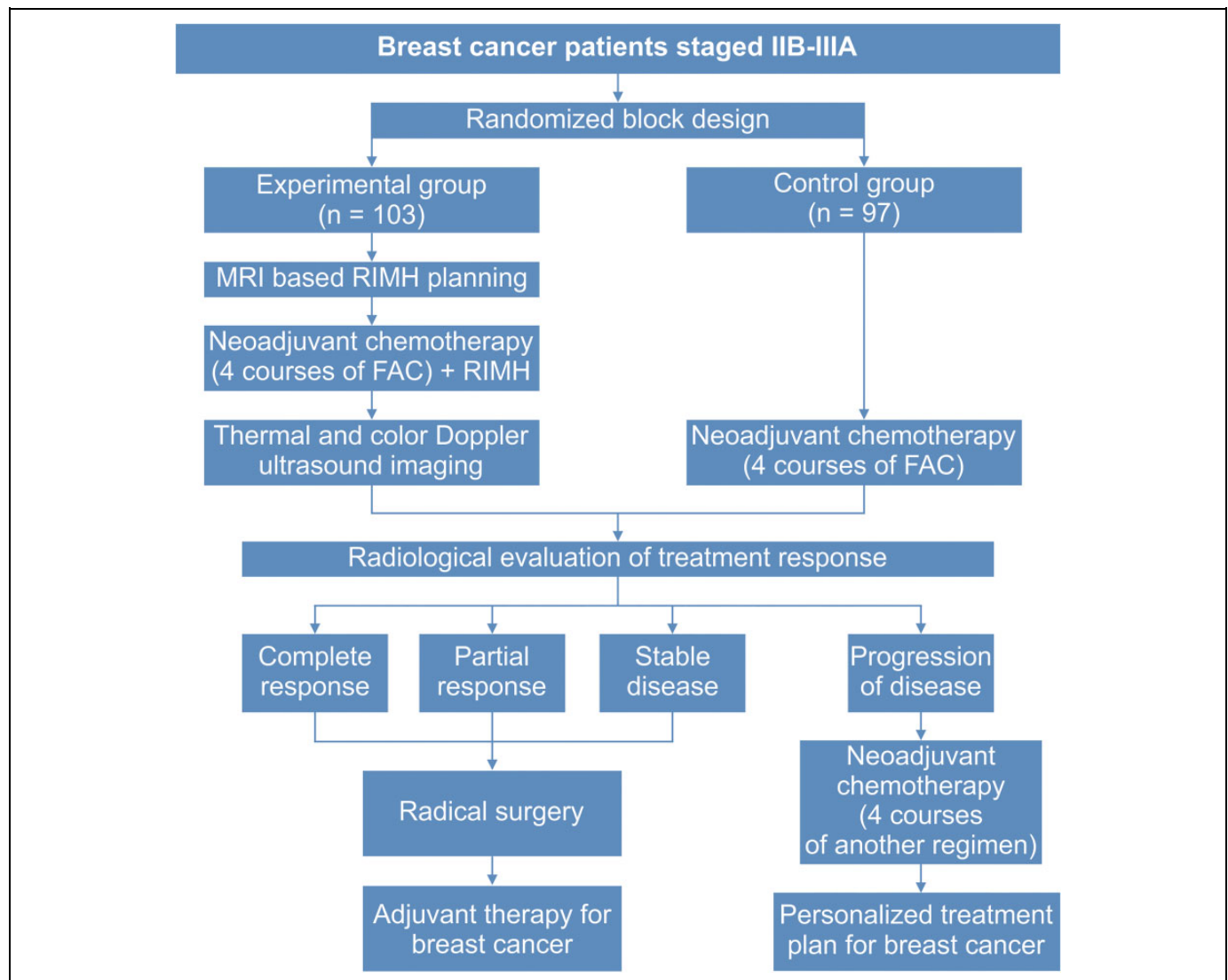


**Figure 1.** Treatment algorithm for patients with locally advanced breast cancer. Abbreviation: FAC, 5-fluorouracil, doxorubicin, cyclophosphamide; MRI, Magnetic resonance imaging; RIMH, Regional inductive moderate hyperthermia.

mammography taken in mediolateral oblique and craniocaudal projections, breast and axillary ultrasound (US), breast magnetic resonance imaging (MRI), computed tomography (CT). Tumor tissue slides were obtained from the pre-treatment trephine biopsy and surgical specimens to carry out hematoxylin and eosin staining for standard histological examination under a light microscope (Zeiss Axiostar Plus, Germany).<sup>18</sup> Immunohistochemistry based estrogen receptor, progesterone receptor, human epidermal growth factor 2 receptor (HER-2) were assessed in all patients.<sup>19</sup>

### Treatments

The control group received 4 courses of neoadjuvant 5-fluorouracil 500 mg/m<sup>2</sup>, doxorubicin 50 mg/m<sup>2</sup>, cyclophosphamide 500 mg/m<sup>2</sup> (FAC). The patients in the experimental group were given 4 courses of NACT followed by a RIMH session 30

minutes after chemotherapy infusion. MRI-based treatment plans were generated prior to RIMH sessions in the experimental group. Three weeks after completion of NACT or NACT + RIMH, the patients underwent radiological evaluation of treatment response for further disease management. Toxicities were graded according to the Common Terminology Criteria for Adverse Events (NCI-CTCAE) v4.03 using a scale from 1 to 5. Figure 1 provides the treatment algorithm for patients with locally advanced BC.

The most frequent indications for mastectomy (Madden technique) with or without immediate reconstruction were stable disease and disease progression. The patients who had achieved a partial or complete response and negative margin resection were candidates for quadrantectomy with simultaneous axillary dissection. Subcutaneous mastectomy and immediate reconstruction were performed on patients with tumors in the central quadrant or multifocal microcalcification.



**Figure 2.** The main applicator (1) and the additional applicator (2) over the tumor in a patient with locally advanced breast cancer during a 30-minute regional inductive moderate hyperthermia session.

Either the modified radical or subcutaneous mastectomy was indicated for BC patients with positive margins at the resection.<sup>20,21</sup> After having assessed the clinical benefit of patients, adjuvant therapy was prescribed in agreement with.<sup>22</sup> The patients were followed according to National Comprehensive Cancer Network (NCCN) Clinical Practice Guidelines version 3.2020 for invasive BC.

### Technology of Regional Inductive Moderate Hyperthermia

Based on our earlier study,<sup>11</sup> the breast and the axilla were being simultaneously irradiated with a MagTherm system (Radmir, Ukraine) at  $27.12 \pm 0.16$  MHz and the 50 W output power for 30 minutes in patients assigned to the experimental group after NACT infusion. The MagTherm applicators were placed parallel to the patient's body over the tumor to produce the highest intensity of electromagnetic radiation. The main applicator (1) had an ellipsoidal shape with a size of  $14 \times 22$  cm placed on the breast, whereas the additional applicator (2) had a size comparable with the tumor (Figure 2). The use of RIMH had a distinct advantage of delivery and absorption in the tumor over other treatment modalities. RIMH was contraindicated in patients who had a fever; acute inflammation; heart failure; respiratory failure, the presence of metallic foreign bodies; pregnancy; epilepsy; complicated ulcer; exacerbation of mental illness; liver and kidney failure; etc.

Computer-assisted planning allowed us to select a personalized distribution of the magnetic, electric and thermal fields generated by RIMH with an individual anatomical precision. MRI-based breast tumor models were created in 2D program SolidWorks. At the time of MRI acquisition and RIMH treatment, the patients were positioned supine. The models for electromagnetic and temperature distribution were built in COMSOL Multiphysics (COMSOL Inc., USA) based on physical characteristics listed in Table 1.<sup>23,24</sup>

The intratumor temperature was predicted to increase from  $37^\circ\text{C}$  to  $38.85^\circ\text{C}$ , while the mean value for the specific absorption rate (SAR) was 5.5 W/kg during the treatment session (Figure 3). Along with the tumor, the parameters of

**Table 1.** Physical Characteristics of the Breast.

Element	Parameters	
	Characteristic	Value
Skin	heat capacity at constant pressure	3391 [J/(kg*K)]
	density	1109 [kg/m <sup>3</sup> ]
	thermal conductivity	0.37 [W/(m*K)]
Breast	electrical conductivity	0.5 [S/m]
	heat capacity at constant pressure	4200 [J/(kg*K)]
	density	1080 [kg/m <sup>3</sup> ]
	thermal conductivity	0.48 [W/(m*K)]
Tumor	electrical conductivity	0.2 [S/m]
	heat capacity at constant pressure	4200 [J/(kg*K)]
	density	1090 [kg/m <sup>3</sup> ]
	thermal conductivity	0.49 [W/(m*K)]
	electrical conductivity	1.5 [S/m]

electromagnetic irradiation for axillary lymph nodes were also computed: the average temperature of  $37.2^\circ\text{C}$  and SAR of 0.59 W/kg. RIMH planning found that the breast tumor heated at nearly  $39^\circ\text{C}$  was more beneficial since moderate hyperthermia would not upregulate the expression of heat-shock proteins in the BC cell, nor restrict blood flow to the tumor. Note that chemotherapy resistance was previously reported at temperatures above  $42^\circ\text{C}$ .<sup>25</sup>

### Imaging Techniques and Analysis

A FLIR thermal imaging camera (FLIR Therma CAMTM E 300) and fiber optical thermometers (TM-4, Radmir, Ukraine) were used for monitoring tumor temperatures during RIMH.

Doppler measurement of velocity combined with B-mode measurement of vessel diameter and tissue harmonic imaging was performed using a NEMIO XG (Toshiba) US scanner with a micro-convex transducer (3.5-5.0 MHz) according to the standard protocol for breast US. Doppler measurements of the peak systolic and end-diastolic velocities provided data about breast tissue vascularity. The examination was performed before NACT + RIMH and 30 minutes after treatment.

Breast MRI scans were acquired on a 1.5 T Intera system (Philips Medical Systems, the Netherlands) following the standard protocol for breath-hold sequences.

Chest CT images (Brilliance Big Bore, Philips Healthcare) were acquired in accordance with the standard protocol for BC patients.

Collected medical images were independently presented to selected radiologists, who were blinded to treatment and any clinical data except that the patients had BC. Two radiologists interpreted each case according to the Response Evaluation Criteria in Solid Tumors (RECIST 1.0).

### Statistical Analysis

Statistical significance was determined using the 2-tailed *t* tests ( $p < 0.05$ ) as appropriate. The Kolmogorov-Smirnov test examined if the data were normally distributed. Overall survival was

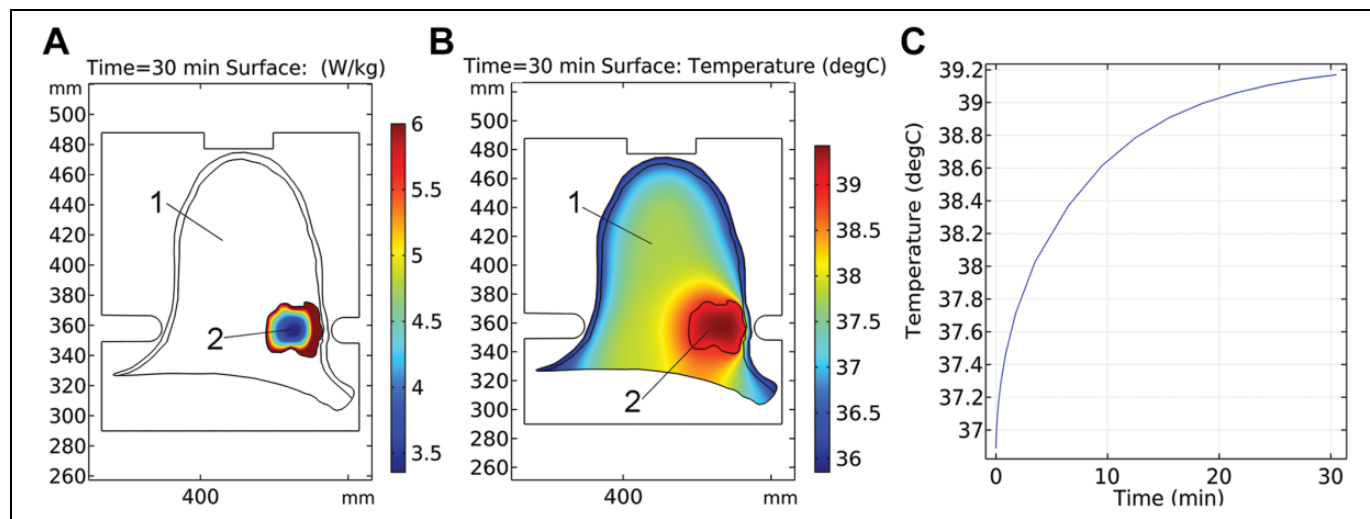


**Figure 3.** The specific absorption rate (A), temperature distribution (B) and temperature rise (C) for breast cancer treatment planning with a MagTherm system at 50 W output power were based on an axial magnetic resonance imaging scan (axes in mm). 1—breast; 2—tumor.

**Table 2.** Patients and Tumor Characteristics.

Parameter	Group		p
	Experimental (NACT and RIMH), n = 103	Control (NACT), n = 97	
Mean age (29-78) years	51.89 ± 9.44	51.03 ± 10.04	> 0.05
Disease stage (NCCN), n (%)			
IIB (T2-3 N0-1M0)	68 (66.02 ± 4.67)	56 (57.73 ± 5.02)	> 0.05
IIIA (T2-3N1-2M0)	35 (33.98 ± 4.67)	41 (42.27 ± 5.02)	
Histological type (ICD-O-3), n (%)			
Invasive ductal carcinoma	96 (93)	89 (92)	> 0.05
Invasive lobular carcinoma	3 (3)	2 (2)	
Mixed lobular-ductal carcinoma	2 (2)	2 (2)	
Rare breast cancer types	2 (2)	4 (4)	
Tumor subtypes, n (%)			
Luminal A	45 (44)	49 (51)	> 0.05
Luminal B	26 (25)	22 (23)	
HER-2+	20 (19)	14 (14)	
Triple negative	12 (12)	12 (12)	
Tumor size 15-85 mm	40.07 ± 1.85	39.59 ± 1.86	> 0.05

Abbreviation: ICD-O-3, International classification of diseases for oncology 3rd edition; HER-2, Human epidermal growth factor 2 receptor; NACT, Neoadjuvant chemotherapy; NCCN, National Comprehensive Cancer Network; RIMH, Regional inductive moderate hyperthermia.

estimated using the Kaplan-Meier method and treatment groups were compared from the log-rank test ( $p < 0.01$ ). The entropy parameter was a statistical measure of randomness in the image content analysis. CHAOS & IMAGE version 1.0 (NCI)<sup>26</sup> computed Shannon's entropy for obtained thermal images according to.<sup>27,28</sup> All statistical analyses were conducted in Statistica 13.0 (Stat-Soft, Inc, 2015).

## Results

### Patients

200 patients with locally advanced BC stage IIB to stage IIIA were recruited at the Department of breast cancer and reconstructive surgery, NCI between 2008 and 2017, of whom 97 received NACT and 103 who received NACT + RIMH. Patient characteristics were similar between the 2 groups (Table 2). There were 5 patients in the experimental group and 4 patients in the control group who had a different subtype after NACT. Identified subtypes did not have an impact on treatment outcomes nor required changes. Likewise, no significant differences were found in the molecular profiles of treated BC patients between the primary tumor and regional lymph node metastases after surgery. This observation was in agreement with the linear evolution model for BC, where molecular profiles of primary breast tumors matched those of metastases.<sup>29,30</sup>

### Thermal Images and Blood Flow of the Breast

The results of temperature distribution and changes in tumor blood flow before RIMH and after can be compared in Figure 4 and Figure 5. RIMH increased the surface temperature on the breasts to  $< 4^{\circ}\text{C}$  (Figure 4). Despite the fact that we irradiated the right breast and axilla, the temperature increased in both breasts and axillae. Axillary lymph node status was of great clinical significance in BC prognosis.<sup>31</sup> The entropy parameter computed for BC thermal images was decreased in both breasts by 10% on average after RIMH.

Color Doppler US examinations were recorded to assess blood flow in the breasts in the experimental group (Figure 5). RIMH significantly increased the number of color signals detected through the blood vessels in the breast tissue. The blood flow rate increased from 44.58 cm/s to 192.78 cm/s after treatment. The mean values for systolic blood flow were 3.5 times as high as those prior to the RIMH session. Similarly, the

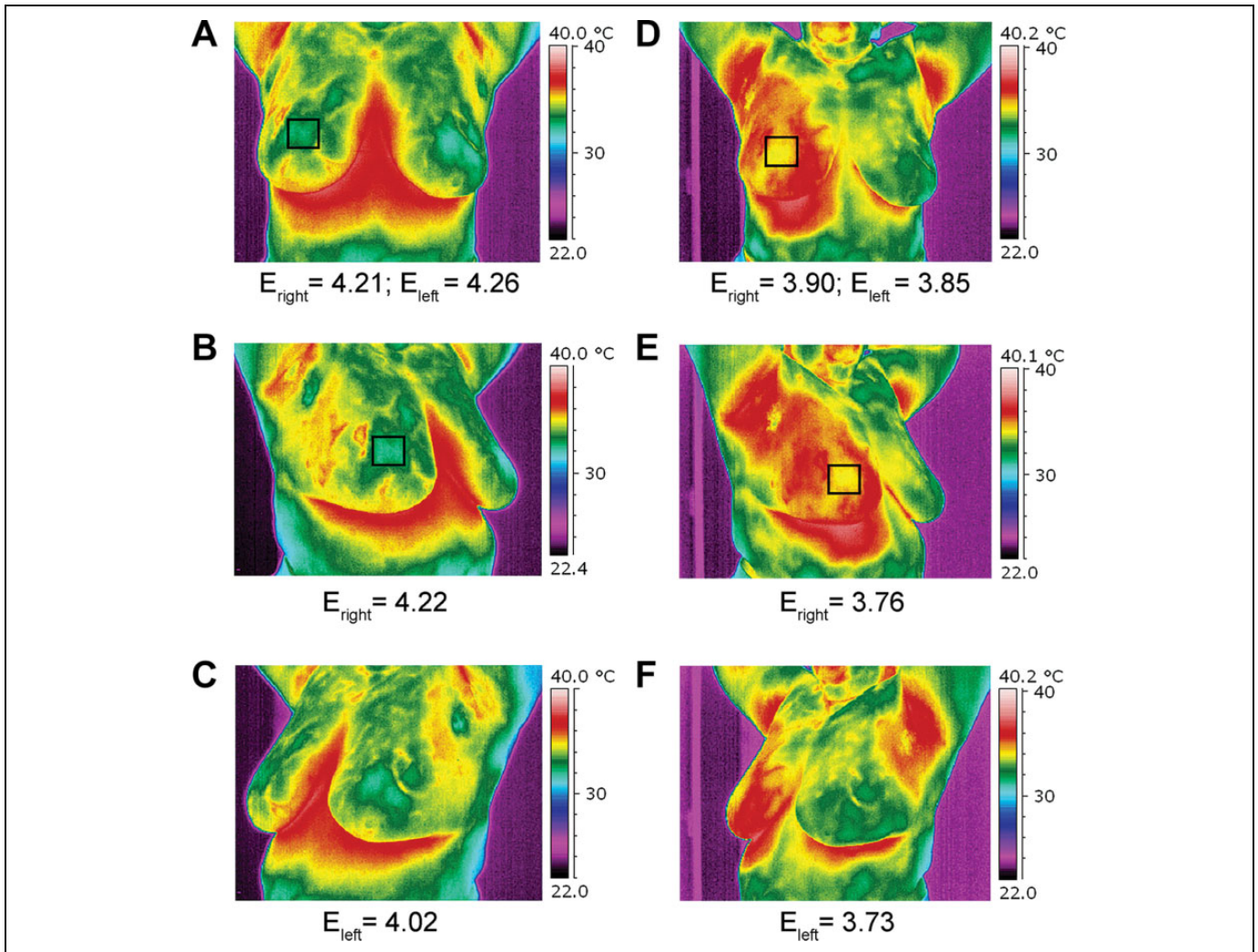


**Figure 4.** Thermal images of a patient with locally advanced breast cancer taken before regional inductive moderate hyperthermia (A, B, C) and after (D, E, F) the treatment session. The entropy (E, arb. units) parameter is computed for obtained images. The tumor is highlighted with the black square. A, D—frontal view; B, E—right oblique view; C, F—left oblique view.

mean diastolic blood flow tended to raise after RIMH. Doppler signals from tumor vasculature were more variable due to spatio-temporal heterogeneity of breast tumors.

### Treatment Response

Tumor response rates are summarized in Table 3. Assessment of tumor size found a  $(31.24 \pm 3.85)\%$  reduction in the size of the primary tumor in patients receiving NACT combined with RIMH, while NACT alone showed a  $(22.95 \pm 3.61)\%$  decrease on average ( $p = 0.034$ ). The objective response was achieved in 58.2% of the patients assigned to the experimental group as compared with 42.3% in the control group ( $p = 0.034$ ).

Thus, NACT combined with RIMH increased the rate of objective response by 15.9% ( $p = 0.034$ ) in patients with locally advanced BC.

There were no significant differences in the size of regional lymph nodes between the 2 groups prior to any treatment procedures. The combination of NACT and RIMH showed a decrease of 7.67 mm ( $32.08 \pm 4.13\%$ ) in the size of the involved lymph nodes, whereas BC patients given NACT alone had a 5.79 mm ( $17.91 \pm 4.35\%$ ) reduction on average. Figure 6 presents a typical case of the lymph node reduction in a BC patient treated with NACT + RIMH. There was a 14.17% difference in the treatment response of axillary lymph node metastasis between NACT followed by RIMH and NACT alone ( $p = 0.011$ ).

Comparing parameters of hematological, gastrointestinal toxicities, liver and kidney function, there was no significant difference between the experimental and the control group. Treatment-induced changes in hematopoiesis and liver function did not represent dose-limiting effects on the prescribed NACT regimen and NACT combined with RIMH in locally advanced BC patients. Moreover, the combination treatment

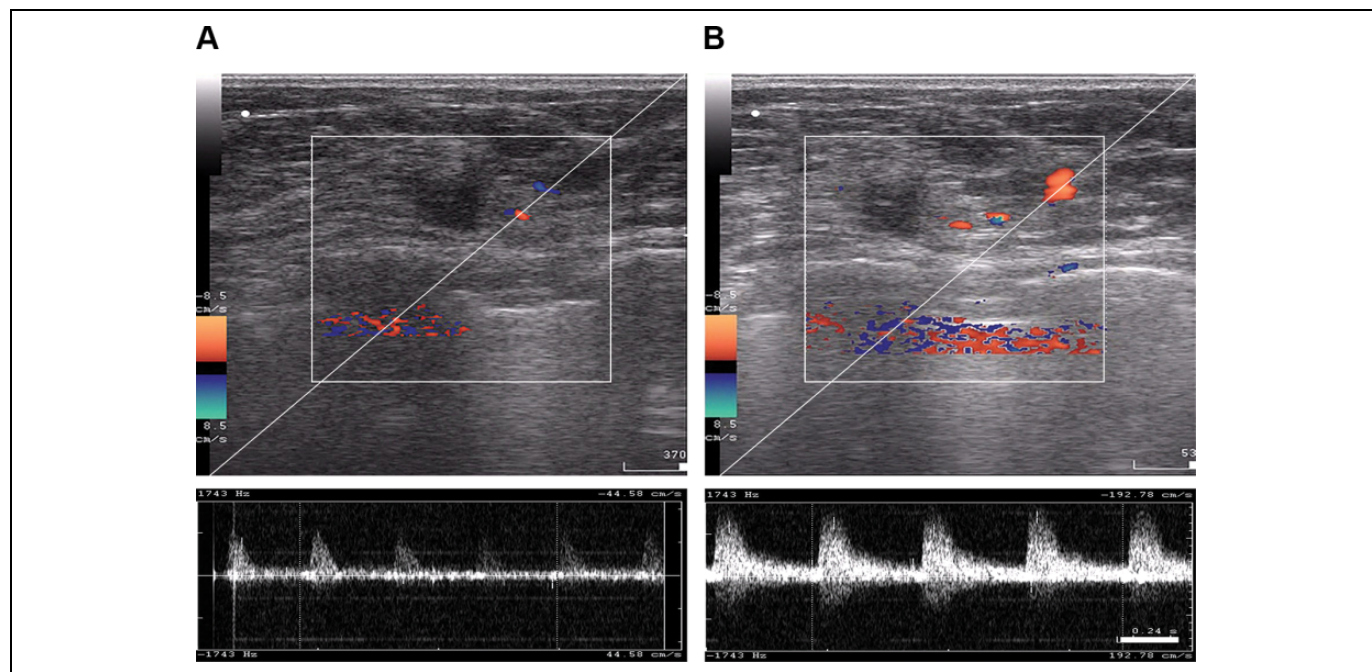


**Figure 5.** B-mode and color Doppler ultrasound imaging of tumor blood flow acquired from a patient with locally advanced breast cancer before regional inductive moderate hyperthermia (A) and 30 minutes after (B) treatment.

**Table 3.** Tumor Response to Treatment According to RECIST.

Response rate (RECIST 1.0)	Group, n (%)				p
	Experimental (NACT + RIMH)		Control (NACT)		
	IIB stage	IIIA stage	IIB stage	IIIA stage	
Complete response	9 (8.7 ± 2.8)	1 (2.9 ± 2.8)	6 (6.2 ± 2.4)	2 (4.9 ± 3.4)	0.68
Partial response	8 (11.8 ± 3.9)	51 (49.5 ± 4.9)	4 (7.1 ± 3.4)	35 (36.1 ± 4.9)	0.076
Stable disease	31 (45.6 ± 6.0)	20 (57.1 ± 8.4)	27 (48.2 ± 3.9)	8 (19.5 ± 6.2)	0.052
Disease progression	37 (35.9 ± 4.7)	14 (40.0 ± 8.3)	49 (50.5 ± 5.1)	7 (7.2 ± 2.6)	0.91
Total	6 (8.8 ± 3.4)	0 (0)	7 (12.5 ± 4.4)	0 (0)	
Total in each stage	103 (100.0)	35 (100)	97 (100.0)	41 (100)	

Abbreviation: NACT, Neoadjuvant chemotherapy; RECIST, Response evaluation criteria in solid tumors v.1.0; RIMH, Regional inductive moderate hyperthermia.

allowed to increase the proportion of women eligible for breast-conserving and reconstructive surgery by 13.63% in the experimental group. Histological changes in tumor tissue treated with NACT and NACT + RIMH are shown in Figure 7.

The 10-year overall survival was significantly higher in BC patients who underwent NACT combined with RIMH than in patients receiving NACT alone at the long-rank  $p < 0.009$  level (Figure 8). There was a significant difference in the 5-year overall survival rate of stage IIB patients between the experimental group (81.7%) and the control group (79.0%),  $p < 0.05$ . We also recorded a significant difference between the overall survival

rates for patients with stage IIIA between the experimental group and the control group: 65.9% and 42.4% at 6 years and 51.1% and 19.8% at 9 years ( $p < 0.05$ ), respectively.

## Discussion

A discussion of the main clinical findings is provided in this section. As is well known abnormal vasculature and growth give rise to the heterogeneous distribution of anoxic, hypoxic and normoxic regions within the tumor and its microenvironment which poses a potent barrier to chemotherapy. There are 2

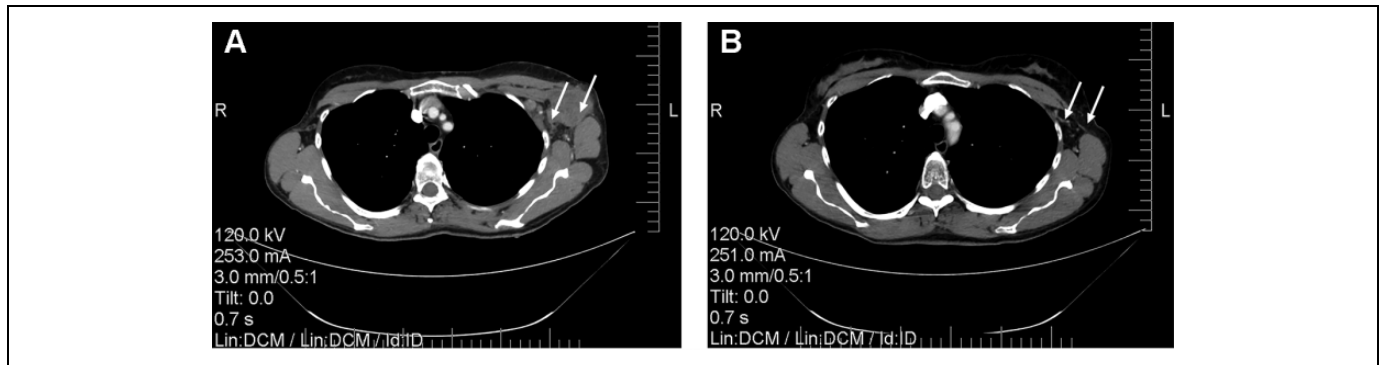


**Figure 6.** Computed tomography scans of the chest showing reduction of axillary lymph node metastasis in a 47-year-old patient who received NACT combined with RIMH: A—before combined treatment; B—after combined treatment. White arrows indicate axillary lymph node metastasis. Abbreviation: NACT, Neoadjuvant chemotherapy; RIMH, Regional inductive moderate hyperthermia.

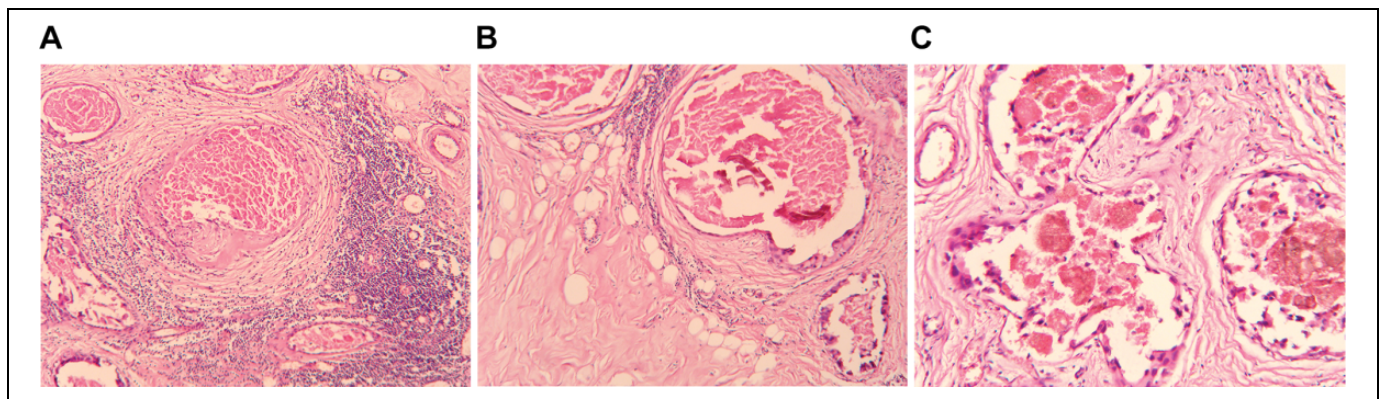


**Figure 7.** Compares tumor histology changes in response to NACT and NACT + RIMH. The viable tumor volume was lower in patients receiving NACT + RIMH ( $24.4 \pm 0.2\%$ ) compared with those given NACT alone ( $30.4 \pm 0.25\%$ ). A, Invasive ductal carcinoma after NACT combined with RIMH treatment. The stroma contains tumor infiltrating lymphocytes, microvascular thrombosis, focal hemorrhages along with the hyaline material, sclerosis and massive necrosis (hematoxylin and eosin staining; magnification  $\times 100$ ); B, invasive lobular carcinoma after NACT combined with RIMH treatment. The appearance of fibrotic changes, prominent sclerosis and cysts (hematoxylin and eosin staining; magnification  $\times 100$ ); C, invasive mixed lobular-ductal carcinoma after NACT. Microvascular thrombosis, blood “sludge,” focal hemorrhages, depositions of hemosiderin and sclerosis (hematoxylin and eosin staining; magnification  $\times 200$ ). Abbreviation: NACT, Neoadjuvant chemotherapy; RIMH, Regional inductive moderate hyperthermia.

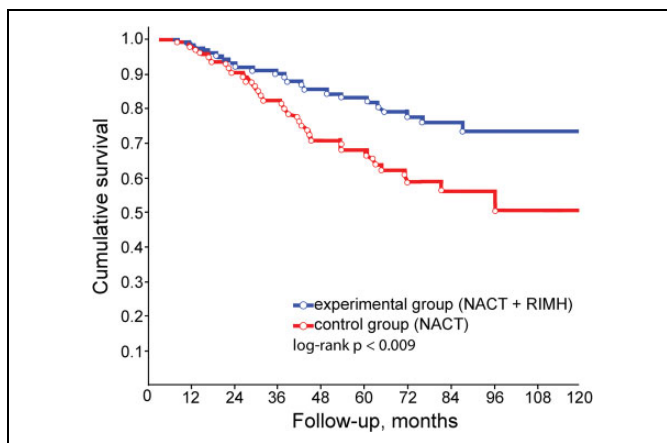


**Figure 8.** 10-year breast cancer survival rates compared from the log-rank test ( $p < 0.009$ ): NACT (control group); NACT combined with RIMH (experimental group). Abbreviation: NACT, Neoadjuvant chemotherapy; RIMH, Regional inductive moderate hyperthermia.

likely causes for this condition: chaotic fluctuations in the tumor perfusion and limitations of oxygen diffusion (i.e., the distance of a tumor cell from the nearest vessels exceeds  $100 \mu\text{m}$ ).<sup>32</sup> Using the combination approach, we suggested synergy between NACT and RIMH to improve the blood flow and hence oxygenation in the tumor.<sup>33</sup>

Having compared the difference between NACT alone and with RIMH, it was shown that 30-minute electromagnetic radiation increased the surface temperature and blood flow to the breast tissue. Acceleration of blood flow through a chaotic vascular network in the breast tumor receiving RIMH with a non-uniform electromagnetic field facilitated more even perfusion which enhanced drug diffusion and microvascular permeability of the tumor.<sup>34</sup> That is, one of the strategies to overcome hypoxia-mediated drug resistance is to increase tumor blood flow.

Histological changes are a strong prognostic factor in solid tumors. They can identify patients at high risk of distant disease



recurrence who benefit from adjuvant therapy.<sup>35</sup> Adverse events were mild (grade 1) and consisted of the well-known side effects for neoadjuvant FAC. Although there was no significant difference between the 2 groups, adverse events tended to reduce in BC patients receiving NACT and RIMH.<sup>36</sup>

The neoadjuvant approach to locally advanced BC can make patients eligible for breast-conserving surgery.<sup>37</sup> Despite the fact that a full discussion of surgical procedures linked with BC lay beyond the main focus of our study, a total of 50.52% of the patients in the control group underwent mastectomy, whereas the rates of mastectomy were decreased to 36.89% in the experimental group. NACT + RIMH treatment also showed an 8.3% increase in the number of patients who were suitable candidates for breast surgery compared with NACT alone ( $p = 0.055$ ). Furthermore, the experimental group had higher rates of breast-conserving surgery than the control group.

The current standard of care for managing locally advanced BC involves removing the primary tumor followed by axillary dissection. Complete lymph node dissection is often associated with a high likelihood of arm lymphedema, loss of motor function and sensory neuropathy.<sup>38</sup> For this reason, it was more beneficial to use NACT + RIMH to achieve the treatment response of axillary lymph node metastasis.

After treatment completion, the 10-year follow-up between 2008-2017 showed that the overall survival was significantly higher in women treated with NACT + RIMH. The treatment outcomes, while preliminary, need to be interpreted as the early-stage experimental results that mirror several mechanisms by which the combination of NACT and RIMH acts on the tumor: (a) tumor heating at 39-40°C prevents the side-effects of the traditional hyperthermia approach such as over-expression of heat shock proteins leading to tumor cell invasion, metastasis and anti-apoptotic pathways associated with chemotherapy resistance<sup>39</sup>; (b) the inhomogeneous electromagnetic field increases blood flow and facilitates more even perfusion to the tumor tissue under which the pulsatile blood flow, shear stress and higher partial oxygen pressure promote oxidative stress arisen from mechano-chemical and magneto-electric redox reactions, thus inducing ROS-mediated apoptosis and necrosis of tumor cells.<sup>40</sup>

## Conclusion

The findings from the present study provided additional clinical evidence that RIMH technology improved the efficacy of NACT given following the standard protocol for patients with locally advanced BC staged IIB-IIIa.

In selected patients NACT combined with RIMH significantly increased the objective response rate, the proportion of women eligible for breast-conserving and reconstructive surgery and the 10-year overall survival rates compared with NACT alone.

Future clinical studies should assess the influence of the proposed RIMH approach on other solid tumors. A natural progression of this work is to develop personalized theranostic

technology integrating magnetic resonance imaging and treatment based on magnetic nanotherapy which will further contribute to improve drug delivery and circumvent chemotherapy resistance in cancer patients.


## Declaration of Conflicting Interests

The author(s) declared no potential conflicts of interest with respect to the research, authorship, and/or publication of this article.

## Funding

The author(s) disclosed receipt of the following financial support for the research, authorship, and/or publication of this article: This work was partially supported by the Ministry of Healthcare of Ukraine.

## ORCID iD

Valerii E. Orel  <https://orcid.org/0000-0002-6319-4215>

## References

1. Surveillance, Epidemiology, and End Results (SEER) Program of the U.S. National Cancer Institute web site. Published 2010-2016. Accessed May 1, 2020. <https://seer.cancer.gov/statfacts/html/breast.html>
2. Siegel RL, Miller KD, Jemal A. Cancer statistics. *Cancer J Clin*. 2019;69(1):7-34. doi:10.3322/caac.21551
3. Polyak K. Heterogeneity in breast cancer. *J Clin Invest*. 2011; 121(10):3786-3788. doi:10.1172/JCI60534
4. Cai K., Xu He N, Singh A, et al. Breast cancer redox heterogeneity detectable with chemical exchange saturation transfer (CEST) MRI. *Mol Imaging Biol*. 2014;16(5):670-679. doi:10.1007/s11307-014-0739-y
5. Brown NS, Bicknell R. Hypoxia and oxidative stress in breast cancer: oxidative stress: its effects on the growth, metastatic potential and response to therapy of breast cancer. *Breast Cancer Res*. 2001;3(5):323-327. doi:10.1186/bcr315
6. Hecht F, Pessoa CF, Gentile LB, Rosenthal D, Carvalho DP, Fortunato RS. The role of oxidative stress on breast cancer development and therapy. *Tumour Biol*. 2016;37(4):4281-4291. doi:10.1007/s13277-016-4873-9
7. Harbeck N, Penault-Llorca F, Cortes J, Gnant M, Houssami N, Poortmans P. Breast cancer. *Nat Rev Dis Primers*. 2019;5(1):66. doi:10.1038/s41572-019-0111-2
8. Mahdavi H. Radiation oncologists' perspectives on reducing radiation-induced heart disease in early breast cancer. *Curr Probl Cancer*. 2020;44(2):100509. doi:10.1016/j.currprobcancer.2019.100509
9. Gorrini C, Harris IS, Mak TW. Modulation of oxidative stress as an anticancer strategy. *Nat Rev Drug Discov*. 2013;12(12):931-947. doi:10.1038/nrd4002
10. Greenebaum B, Barnes F. *Biological and Medical Aspects of Electromagnetic Fields*. 4th ed. CRC Press; c2018:1-649. doi:10.1201/9781315186641
11. Orel VE, Kudryavets YI, Satz S, et al. Mechanochemically activated doxorubicin nanoparticles in combination with 40 MHz frequency irradiation on A-549 lung carcinoma cells. *Drug Deliv*. 2005;12(3):171-178. doi:10.1080/10717540590932007

12. Orel VE, Tselepi M, Mitrelias T, et al. Nonlinear magnetochemical effects in nanotherapy of Walker-256 carcinosarcoma. *ACS Applied Bio Mater.* 2019; 2(9):3954-3963. doi:10.1021/acsabm.9b00526
13. Sampson C, Keens RH, Kattnig DR. On the magnetosensitivity of lipid peroxidation: two- versus three-radical dynamics. *Phys Chem Chem Phys.* 2019;21(25):13526-13538. doi:10.1039/c9cp01746a
14. Lewis GN. The magnetochemical theory. *Chem Rev.* 1924;1(2): 231-248. doi:10.1021/cr60002a003
15. Dewhirst MW, Lee CT, Ashcraft KA. The future of biology in driving the field of hyperthermia. *Int J Hyperthermia.* 2016;32(1): 4-13. doi:10.3109/02656736.2015.1091093
16. Liou GY, Storz P. Reactive oxygen species in cancer. *Free Radic Res.* 2010;44(5):479-496. doi:10.3109/10715761003667554
17. Klimanov MYu, Syvak LA, Orel VE, et al. Efficacy of combined regional inductive moderate hyperthermia and chemotherapy in patients with multiple liver metastases from breast cancer. *Technol Cancer Res Treatment.* 2018;17:1-7. doi:10.1177/1533033818806003
18. Bancroft JD, Layton C. The hematoxylin and eosin. In: Suvarna SK, Layton C, Bancroft JD, eds. *Theory and Practice of Histological Techniques.* 8th ed. Elsevier; 2019:126-139. doi:10.1016/C2015-0-00143-5
19. Weigelt B, Geyer FC, Reis-Filho JS. Histological types of breast cancer: how special are they? *Mol Oncol.* 2010;4(3):192-208. doi: 10.1016/j.molonc.2010.04.004
20. Volders JH, Negenborn VL, Sponk PE, et al. Breast-conserving surgery following neoadjuvant therapy—a systematic review on surgical outcomes. *Breast Cancer Res Treat.* 2018;168(1):1-12. doi:10.1007/s10549-017-4598-5
21. Veronesi U, Cascinelli N, Mariani L. More long-term data for breast-conserving surgery. *N Engl J Med.* 2002;347(16): 1227-1232. doi:10.1056/nejmoa020989
22. Miller E, Lee HJ, Lulla A, Hernandez L, Gokare P, Lim B. Current treatment of early breast cancer: adjuvant and neoadjuvant therapy. *F1000Res.* 2014;3:198. doi:10.12688/f1000research.4340.1
23. Bardati F, Iudicello S. Modeling the visibility of breast malignancy by a microwave radiometer. *IEEE Trans Biomed Eng.* 2008;55(1):214-221. doi:10.1109/TBME.2007.899354
24. Russel KH, Bradley JR. *Intermediate Physics for Medicine and Biology.* Springer Science; c2007:1-616. doi:10.1007/978-0-387-49885-0
25. Song CW. Effect of local hyperthermia on blood flow and micro-environment: a review. *Cancer Res.* 1984;44(10):4721s-4730s.
26. Orel V, Kozarenko T, Galachin K, Romanov A, Morozoff A. Nonlinear analysis of digital images and Doppler measurements for trophoblastic tumor. *Nonlinear Dynamics Psychol Life Sci.* 2007;11(3):309-331.
27. Sparavigna AC. Entropy in image analysis. *Entropy.* 2019;21(5): 502. doi:10.3390/e21050502
28. Julio MR, José VN, Horacio LA, Diego PR, Santiago GG, Miguel GT. Entropy and contrast enhancement of infrared thermal images using the multiscale top-hat transform. *Entropy.* 2019; 21(3):244. doi:10.3390/e21030244
29. Carey LA, Perou CM, Livasy CA, et al. Race, breast cancer subtypes, and survival in the Carolina Breast Cancer Study. *JAMA.* 2006;295(21):2492-2502. doi:10.1001/jama.295.21.2492
30. Chen R, Goodison S, Sun Y. Molecular profiles of matched primary and metastatic tumor samples support a linear evolutionary model of breast cancer. *Cancer Res.* 2020;80(2):170-174. doi:10.1158/0008-5472.CAN-19-2296
31. Hung M, Xu J, Nielson D, et al. Evaluating the prediction of breast cancer survival using lymph node ratio. *J Breast Cancer.* 2018;21(3):315-320. doi:10.4048/jbc.2018.21.e35
32. Grimes DR, Kannan P, Warren DR, et al. Estimating oxygen distribution from vasculature in three-dimensional tumour tissue. *J R Soc Interface.* 2016;13(116):20160070. doi:10.1098/rsif.2016.0070
33. Dewhirst MW. Concepts of oxygen transport at the microcirculatory level. *Semin Radiat Oncol.* 1998;8(3):143-150. doi:10.1016/s1053-4296(98)80040-4
34. Dewhirst MW, Secomb TW. Transport of drugs from blood vessels to tumour tissue. *Nat Rev Cancer.* 2017;17(12):738-750. doi: 10.1038/nrc.2017.93
35. Wu J, Liang C, Chen M, Su W. Association between tumor-stroma ratio and prognosis in solid tumor patients: a systematic review and meta-analysis. *Oncotarget.* 2016;7(42):68954-68965. doi:10.18632/oncotarget.12135
36. US Department of Health and Human Services, National institutes of Health National Cancer Institute. Common Terminology Criteria for Adverse Events (CTCAE) version 4.0. 2009 (v 4.03: June 14, 2010).
37. Thompson AM, Moulder-Thompson SL. Neoadjuvant treatment of breast cancer. *Ann Oncol.* 2012;23(Suppl 10):x231-x236. doi: 10.1093/annonc/mds324
38. Costin AI, Păun I, Vârcaș F, et al. Intraoperative assessment of sentinel lymph nodes in early-stage breast cancer. *Rom J Morphol Embryol.* 2018;59(4):1033-1039.
39. Wu J, Liu T, Rios Z, Mei Q, Lin X, Cao S. Heat shock proteins and cancer. *Trends Pharmacol Sci.* 2016;38(3):226-256. doi:10.1016/j.tips.2016.11.009
40. Saikolappan S, Kumare B, Shishodia G, Koulb S, Koul HK. Reactive oxygen species and cancer: a complex interaction. *Cancer Lett.* 2019;452(28):132-143. doi:10.1016/j.canlet.2019.03.020